Biochimica et Biophysica Acta 1818 (2012) 49–54

Contents lists available at SciVerse ScienceDirect

Biochimica et Biophysica Acta

journal homepage: www.elsevier.com/locate/bbamem

Structural basis for misfolding at a disease phenotypic position in CFTR: Comparison of TM3/4 helix-loop-helix constructs with TM4 peptides

Cory M. Mulvihill, Charles M. Deber *

Division of Molecular Structure and Function, Research Institute, Hospital for Sick Children, Toronto, Ontario, Canada M5G 1X8
Department of Biochemistry, University of Toronto, Toronto, Ontario, Canada M5S 1A8

ARTICLE INFO

Article history:
Received 11 July 2011
Received in revised form 15 September 2011
Accepted 26 September 2011
Available online 3 October 2011

Keywords:
Cystic fibrosis transmembrane conductance regulator (CFTR)
Hydropathy
Membrane protein
SDS-PAGE

ABSTRACT

Understanding the residue-dependent effects of disease-phenotypic mutations in multi-spanning membrane proteins is an essential step toward the development of corrective therapies. As a systematic approach to further elucidate mutant-dependent mis-folding consequences, we prepared two libraries: one consisting of 20 helix-loop-helix ("hairpin") constructs derived from helices 3 and 4 of the human cystic fibrosis transmembrane conductance regulator (CFTR) (residues 194–241) in which the CF-phenotypic position Val-232 was substituted individually to each of the 20 commonly-occurring amino acids; and a second library consisting of 20 single-stranded TM4 peptides (CFTR residues 221–241) similarly substituted at position 232. Both libraries were analyzed to measure mutant-dependent variations in mobility on SDS-PAGE; size and shape on size exclusion chromatography; retention times on reverse phase HPLC; and helical content by circular dichroism spectroscopy. Analysis of a scatter plot between TM3/4 hairpin and TM4 peptide retention times showed a strong correlation ($r = 0.94$, $p < 0.05$), with retention times largely a function of residue hydrophobicity. In contrast, while the hairpin library migrated over a significant range on SDS-PAGE, migration rates for TM4 hydrophobic residues at position 232 converged at a single value, suggesting that residue-dependent re-orientations of hairpin van der Waals interfaces may expose varying faces of the TM3 and/or TM4 helices to the SDS detergent. The overall results suggest that mutant-mediated variations are a principal determinant of tertiary interhelical folding interactions in membranes.

1. Introduction

Deciphering how a particular mutation may affect folding of a membrane protein at either the initial membrane insertion step, or in determining the nature and strength of association between transmembrane (TM) helices in a subsequent folding step, would provide an essential foundation for the development of corrective therapies for diseases that arise from point mutations in multi-spanning membrane proteins [1]. While significant advances have been made in the prediction of initial translocon-mediated helix insertion [2–7], the ability to predict the subsequent step in folding, *i.e.*, the creation and specific nature of tertiary helix–helix interactions, is less well-understood. Using the Popot and Engelman two-stage membrane protein folding model as a guide [8], one can endeavor to deconstruct the specific amino acid contributions to each of these steps. In previous work, we probed the first stage of this process, translocon-mediated insertion [9]. We discovered through the analysis of a helical protein model that reverse phase-high performance liquid chromatography (RP-HPLC) can assess the hydropathy of a segment much in the way as does the translocon. These findings tended to support the notion that the translocon acts as a passive facilitator of helix insertion into the membrane bilayer that can detect a threshold level of hydropathy of the segment through allowing helix–lipid interactions to be sampled.

The present work now aims to systematically examine the residue-specific influences on helix–helix interactions through the generation of a library of helix-loop-helix segments (transmembrane segments 3 and 4) of the cystic fibrosis transmembrane conductance regulator (CFTR) – the minimal model that will allow us to probe tertiary interactions – substituted with each of the 20 commonly occurring amino acids at a single CF-phenotypic site in TM4 (Val-232). Biophysical analyses of these constructs are then compared with a corresponding series of single-stranded TM4 peptide models containing each of the 20 amino acids substituted individually at the corresponding TM4 position. The results provide insights into the sequence-dependent ability of the hairpin model to form helix–helix contacts.

Abbreviations: CD, circular dichroism; CFTR, human cystic fibrosis transmembrane conductance regulator; ESI-MS, electron spray ionization-mass spectrometry; HPLC, high performance liquid chromatography; MALDI, matrix assisted laser desorption ionization-mass spectrometry; MES, 2-(*N*-morpholino)ethanesulfonic acid; MRE, mean residue ellipticity; RP, reverse phase; SDS-PAGE, sodium dodecyl sulfate-polyacrylamide gel electrophoresis; SEC, size exclusion chromatography; TFA, trifluoroacetic acid; TM, transmembrane

* Corresponding author at: Division of Molecular Structure and Function, Research Institute, Hospital for Sick Children, 555 University Avenue Toronto, Ontario, Canada M5G 1X8. Tel.: +1 416 813 5924; fax: +1 416 813 5005.
E-mail address: deber@sickkids.ca (C.M. Deber).

0005-2736/$ – see front matter © 2011 Elsevier B.V. All rights reserved.
doi:10.1016/j.bbamem.2011.09.027

2. Materials and methods

2.1. Protein expression and purification

TM3/4 hairpins were expressed and purified as previously described [10,11] with the sequence: GSGMKETAAAKFERQHMDSPDLGTDDDD-KAM**GLALAHFVWIAPLQVALLMGLIWELLQASAFAGLGFLIXLALFQAGL-G**LEHHHHHH, where bold text indicates the CFTR fragment and mutated residue X is underlined. Mutations at position 232 that coded for each of the twenty natural amino acids were generated by use of the QuikChange site-directed mutagenesis kit (Stratagene). Nickel affinity chromatography was used to purify constructs from BL21(DE3) cells followed by removal of the solubilization domain with thrombin cleavage and final purification using a C4 RP-HPLC gradient of acetonitrile prior to lyophilization to obtain pure hairpin, as determined by the HPLC chromatogram, mass spectrometry analysis and SDS-PAGE analysis.

2.2. Peptide synthesis and purification

Peptides of CFTR transmembrane four (TM4) amino acids 221–241 with sequence: H_2N-KKASAFAGLGFLIXLALFQAGLGKK-NH_2 were synthesized via Fmoc chemistry on a PS3 peptide synthesizer (Protein Technologies, Inc.). Peptide solubility was enhanced by the addition of two lysine residues to each of the N- and C-termini [12]. Low load Fmoc-PAL-polyethylene glycol-polystyrene resin (Applied Biosystems) was used for incorporation of a C-terminal amide group on the final product. Synthesis was performed at a 0.4 mmol scale to residue 233 then divided into four to incorporate each mutant at the 0.1 mmol scale. The activating pair *O*-(7-azabenzotriazol-1-yl)-*N*,*N*,*N*′,*N*′-tetramethyl-uronium hexafluorophosphate and *N*,*N*-diisopropylethylamine was used in a four-fold molar excess. Cleavage and deprotection of the peptides were completed in a solution of 88% trifluoroacetic acid (TFA), 5% phenol, 5% water and 2% triisopropylsilane. The peptide was isolated from the cleavage solution through precipitation and sequential washes in cold ethyl ether prior to drying and resuspension in water. Final purification was completed by reverse phase-high performance liquid chromatography (RP-HPLC) with a C4 preparative column (Phenomenex) in a water/acetonitrile gradient with the presence of 0.1% TFA. Molecular weight and purity were assessed by mass spectrometry and SDS-PAGE analysis.

2.3. Construct identification and quantitation

Expected molecular weights of each construct were confirmed by either matrix assisted laser desorption ionization-mass spectrometry (MALDI-MS) or electrospray ionization-mass spectrometry (ESI-MS). The Micro BCA Protein Assay Kit (Thermo Scientific) was used to determine the concentration of TM4 peptides in water using manufacturer's instructions and to determine TM3/4 protein concentrations with standards and samples prepared in 0.3% sodium dodecyl sulfate (SDS), 50 mM sodium phosphate, pH 7.0.

2.4. Circular dichroism (CD) measurements

A Jasco J-810 spectropolarimeter was used to record CD spectra of TM4 peptides. All spectra were obtained at room temperature in 0.3% SDS, 50 mM sodium phosphate, pH 7.0 using a cuvette with 1 mm path length and a peptide concentration of ~30 μM. Each spectrum is an average of three scans using a response time of 4 s, a 2 nm bandwidth and 50 nm/min scan speed between 250 and 190 nm. Spectra were corrected for solvent background signal then converted to mean residue ellipticities (MRE).

2.5. Sodium dodecyl sulfate-polyacrylamide gel electrophoresis (SDS-PAGE) mobility analysis

NuPAGE 12% Bis–Tris gels (Invitrogen) were run in 2-(*N*-morpholino) ethanesulfonic acid (MES) running buffer, pH 7.3 at 140 V to resolve hairpin and peptide mobilities. Samples of 1–2 μg were prepared in lithium dodecyl sulfate-loading buffer and loaded without boiling. Protein visualization was completed using either Coomassie Brilliant Blue (G-250) stain or GelCode Blue Stain Reagent (Thermo Scientific). Mark12 Unstained Standards (Invitrogen) were used for molecular weight estimation. NIH ImageJ [13] was used to measure gel migration distances of samples with the distance determined by the point of highest density in the protein band.

2.6. Analytical size exclusion chromatography

SEC analysis was performed as previously described [14]. Briefly, samples were analyzed using a 7.8 mm × 300 mm BioSep SEC-S2000 column (Phenomenex) equilibrated with 10 volumes of mobile phase: 0.3% SDS, 50 mM sodium phosphate, pH 7. Purified hairpin samples (~300 μg) were pre-equilibrated in mobile phase prior to injection and run at 0.5 mL/min. Retention times were determined by maximum absorbance at 280 nm.

2.7. Reverse phase HPLC analysis

Analytical TM4 peptide retention times were determined with a Vydac 218TP C18 column (Grace Davison Discovery Sciences). The samples were run over an acetonitrile gradient from 20 to 60% in the presence of water and 0.1% TFA. The gradient was run at 3 mL/min over 40 min. The analyte was injected as a 1 mL solution of 20 μg peptide in 20% acetonitrile, 0.1% TFA in water.

3. Results

3.1. Sequence- and conformational-dependence of SDS-PAGE mobility

We expressed and purified a library of 20 hairpins derived from CFTR TM3/4 segments where the CF-phenotypic residue position 232 is substituted with each of the 20 commonly-occurring amino acids. The primarily helical nature of hairpins typical of this library was previously confirmed, satisfying a key prerequisite of a model of polypeptide folding in the lipid bilayer [9]. Previous work in our lab has shown that SDS-PAGE can be used as an effective technique to evaluate hairpin interactions with lipid [10,14,15], as well as its ability to detect changes in migration due to the substitution of a single amino acid in this 87-residue construct. Accordingly, the hairpin library was analyzed by SDS-PAGE, with the resulting mobilities shown in Fig. 1A; although the hairpins have closely similar molecular weights, significant variations in their gel mobilities are apparent. These differences were quantitated by measuring migration distances and show statistically significant variations among mutants that may be ordered relative to WT mobility (Fig. 1B). It is noteworthy that the acidic and polar residue mutants such as Asp, Glu and Asn have the fastest mobilities, while hydrophobic residues such as Leu and Phe have the slowest mobilities. This trend is consistent with previous observations of a direct correlation between increased hydrophobicity and reduced SDS-PAGE mobility in the TM3/4 hairpin system [14]. However, departures in detail from common hydropathy scales suggest that other factors, such as mutant-dependent retention of TM3–TM4 interfacial interactions in SDS, may also be contributors.

3.2. Determining relative hairpin Stokes radius by size exclusion chromatography

As an alternative technique to assess the effects of detergent loading on particle size and shape, size exclusion chromatography (SEC) analysis

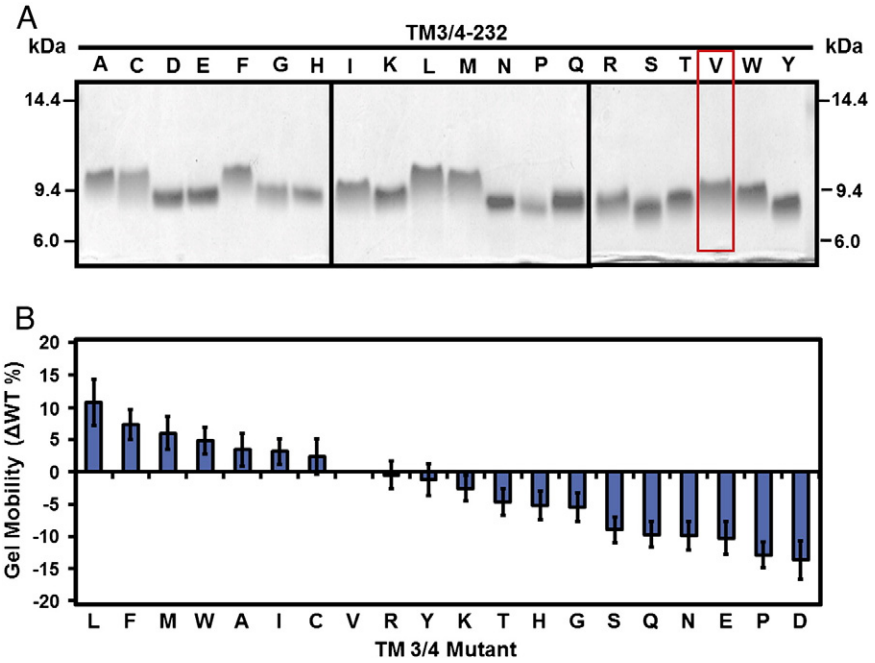

Fig. 1. SDS-PAGE analysis of helical hairpins. (A) Gel mobilities for each of the 20 hairpin mutants. The mutation at position 232, numbered according to the corresponding position within the CFTR transmembrane domain, is indicated at the top of each lane with the wild type V232 outlined in red. (B) Differences in mobilities among mutants were quantitated through migration distance measurements with ImageJ [13] and normalized to percent deviation from wild type V232. Error bars are shown for migration determinations (mean ± SEM, n = 3).

in 0.3% SDS was performed for the library of 20 hairpins. This technique reports the Stokes radius of a particle, a hard sphere model that corresponds to its average hydrodynamic size. Larger Stokes radii therefore do not universally indicate increased mass but may also correspond to species that are altered in shape, such that they are less compact and/or sample a larger volume or range of conformations. However, since all of the hairpins are of closely comparable molecular weights, retention time variations in SEC were expected to report the effects of mutations on some combination of the shape, size, flexibility and/or dynamics of the hairpin–detergent complexes.

SEC analysis was indeed able to identify significant differences among many of the mutant hairpins (Fig. 2A). We noted that those mutants migrating faster than wild type on SDS-PAGE tended to have larger Stokes radii and vice-versa. Mutants displaying smaller Stokes radii than the wild type Val include Leu, Ile and Phe. On the other hand, those with the largest Stokes radii include those with the helix-breaking Pro, acidic Asp, and the polar Asn residue at position 232. When the trend in the SEC values is compared against SDS-PAGE mobilities (Fig. 2B), a strong inverse correlation is observed ($r = 0.88$, $p < 0.05$). While the effect of protein–detergent complex shape on gel mobility is not fully understood, this result suggests that an increase in protein–detergent complex flexibility and/or dynamics among the less hydrophobic mutants may permit more rapid sieving through the gel matrix, even though SEC reports the retention time of an equivalent hard sphere, while SDS-PAGE mobility is determined by a sieving effect through a porous matrix.

3.3. Analysis of TM4 single strand peptides in the absence of potential tertiary folding effects

In order to isolate contributions to SDS-PAGE mobility of CFTR TM3/4 hairpins arising from protein–detergent *vs.* intra-protein contacts, a corresponding library of single TM4-only peptides was synthesized and characterized (Fig. 3A), again with each of the 20 commonly-occurring amino acids substituted at position 232. This set of peptides was first assessed for helical content by circular dichroism (CD) spectroscopy in the presence of SDS micelles (Fig. 3B) and found to be primarily helical, as evidenced by minima at 208 and 222 nm. The observed mutant-dependent range in extent of helicity (*e.g.*, −6160° at 222 nm for the N-232 peptide *vs.* −19,647° for the I-232 peptide) appeared, to a first approximation, to be consistent with an increased level of SDS interaction with the more hydrophobic sequences [14]. Parallel measurements of selected TM4 peptides in water showed spectra typical of unordered structure, confirming that helicity of the peptides is conferred by interaction with SDS (data not shown). TM4 peptide hydropathy was further quantitated by RP-HPLC to determine if it matched the trends seen in the hairpin library. Analysis of a scatter plot between TM4 retention times and previously determined TM3/4 retention times [9] showed a strong correlation of $r = 0.94$ ($p < 0.05$) (Fig. 4).

3.4. Relating TM4 mobility to conformational effects in hairpins

SDS-PAGE analysis was used to determine how mutations at position 232 in the TM4 single strand peptide library affect gel migration in the absence of the ability of the monomeric peptide to form intra-hairpin contacts (Fig. 5A). We found that mutations to hydrophobic residues in TM4 display intermediate, closely comparable migrations, while negatively charged mutants (Asp, Glu) have the fastest mobilities and positively charged mutants (Lys, Arg) have slower mobilities. This latter result is in partial contrast to the trends seen in the TM3/4 hairpin migrations where both positively charged and negatively charged residues had faster mobilities.

To compare the mobilities of the TM4 peptides *vs.* those of the TM3/4 hairpins, gel migration positions for each series were normalized to a scale between −10 and 10, and then plotted on a scatter plot where the line $y = x$ would indicate a perfect agreement in migration variability between the two series (Fig. 5B). A group of hydrophobic residues (Leu, Phe, Met, Ala, Ile and Cys) fell well off the line $y = x$, having little variation among their TM4 peptide mobilities, but displaying significant differences among their hairpin mobilities. However, polar mutations – the acidic Asp and Glu, and the polar residues Asn, Gln, Ser, Thr and His – did fall along the line, suggesting

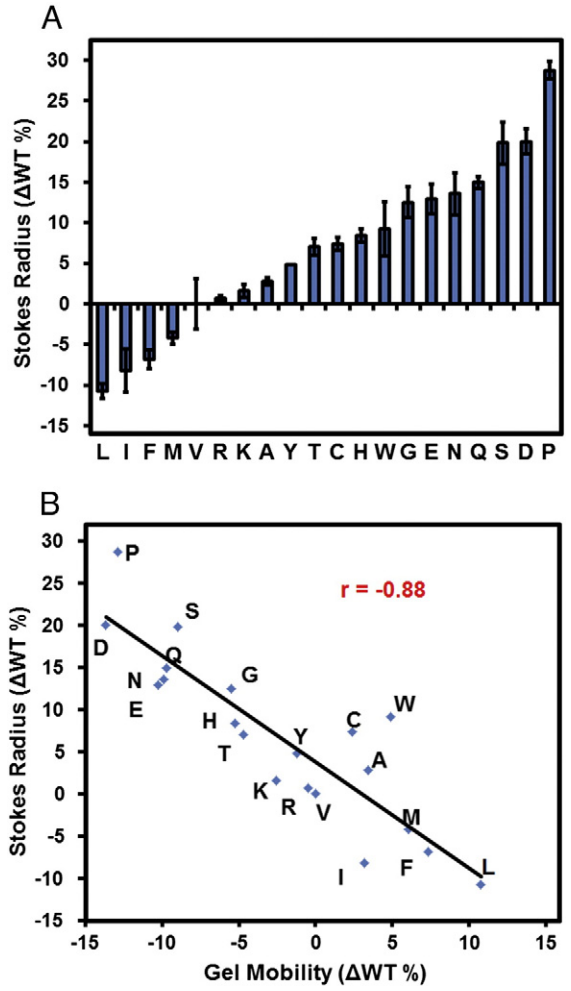

Fig. 2. Analysis of hairpins by size exclusion chromatography. (A) Analytical size exclusion chromatography was used to determine retention times for the hairpin position 232 mutant series. Values are shown as their Stokes radii relative to the wild type V232 (mean ± SEM, n = 3). (B) Hairpin SEC results are shown in a scatter plot against gel mobilities determined in Fig. 1 with the corresponding correlation coefficient shown.

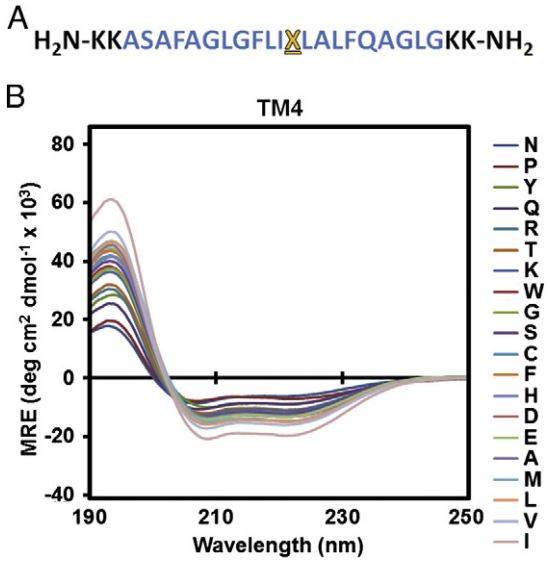

Fig. 3. Circular dichroism spectra of single-stranded TM4 peptide constructs. (A) Amino acid sequence of the designed TM4 peptide with the segment corresponding to TM4 from CFTR rendered in blue. Lysine residues are included at N- and C-termini as 'tags' to aid in peptide synthesis and solubility [12]. The mutated position 232 is highlighted as 'X' in red. (B) The CD spectra of the peptide series were determined in SDS micelles and are shown in order of increasing helicity (n = 3), as indicated to the right of the diagram.

that their mobilities are largely dominated by the reduced SDS binding expected at these acidic and hydrophilic sites [14].

The possibility that the relatively slower mobilities observed for TM4 Lys and Arg peptides was due to the formation of dimers rather than the result of enhanced detergent loading was considered. Lys and Arg residues have the potential to form cation–π interactions [16], but this is unlikely in the absence of a Trp in the TM4 peptide, while two Trp residues occur in the TM3/4 hairpin, including the membrane-embedded W202 in TM3. In addition, to further rule out the possibility of TM4–TM4 dimer formation, selected mutants were also analyzed using a Tris–Glycine gel system which has previously been shown to resolve monomer–dimer populations that were not resolved under the NuPAGE MES system [17]. Examined mutants ran as single bands under both systems, suggesting that mobility variations are not due to dimer formation (data not shown).

4. Discussion

In the present work we have performed biophysical analysis through systematic substitution of CF-phenotypic position Val-232 in a TM3/4 hairpin of human CFTR individually to each of the 20 commonly-occurring amino acids, and compared this library with corresponding single strand TM4 peptides similarly substituted at position 232 with each of the 20 commonly-occurring amino acids. Key approaches involved the use of SDS-PAGE to detect mutant-dependent variations in gel mobility [14], in combination with SEC and RP-HPLC measurements, and secondary structure measurements by CD spectroscopy.

4.1. SDS-PAGE and SEC analysis of TM3/4 hairpins vs. TM4 peptides

Most TM3/4 hairpins substituted with hydrophobic residues displayed comparable or smaller Stokes radii than the wild type V232. However, the relatively slower gel mobilities among this group of mutants is a known consequence of enhanced detergent binding [14] that might be expected to increase the effective size of the protein–detergent particle. These seemingly contradictory results may be rationalized if the volume occupied by the hairpin–detergent particle is influenced by additional factors, such as the packing densities attainable by the TMDs in the TM3/4 construct. For the hydrophobic mutants, it is possible that enhanced detergent 'coating' of these mutants promotes greater particle compactness via intra-hairpin

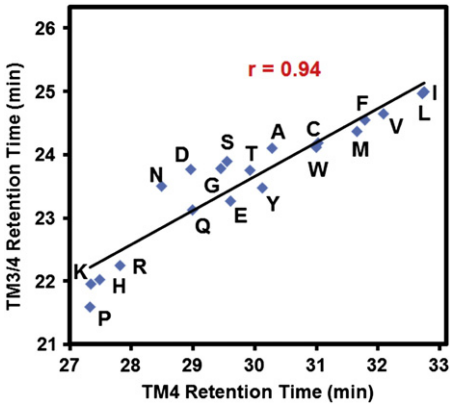

Fig. 4. HPLC retention times of CFTR TM3/4 hairpins *vs.* single-stranded TM4 peptides. RP-HPLC retention times of TM4 peptides were plotted against previously determined retention times for the hairpin series [9] in a water/acetonitrile gradient (see Materials and methods). Data points are identified by the amino acid mutant at position 232. The calculated correlation coefficient r is shown.

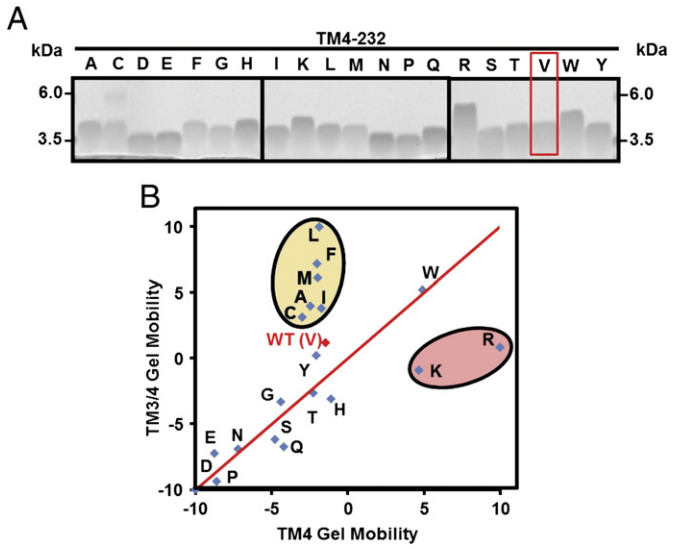

Fig. 5. SDS-PAGE mobilities of CFTR TM3/4 hairpins *vs.* single-stranded TM4 peptides. (A) The gel migration of each mutant in the TM4 peptide series is shown with the position 232 mutant indicated. The wild type V232 is indicated by a red outline. (B) Variations in gel mobilities of the hairpin mutant library *vs.* the corresponding TM4 peptide mutants, normalized to a scale from −10 to 10 and shown in a scatter plot (n = 3). The red line is y = x, the theoretical curve that would represent equal variations in mobility between both series. Shaded ellipses indicate groups of mutants with mobilities that have statistically significant differences from the curve y = x. See text for a further discussion.

packing. In contrast, the absence of a second segment when the single TM4 peptide is considered exposes all residues to detergent interaction without the possibility of masking by TM3–TM4 contacts. As well, by allowing access to an aqueous-exposed surface, the micellar environment allows SDS-PAGE mobility to directly detect the residue-dependent detergent binding around the full periphery of the TM4 single helix [18]. The observed variation in CD ellipticity values of the TM4 peptide library supports the latter contention, as the amount of SDS bound to the segment is known to influence helicity [14].

4.2. Toward a predictive scale for helix–helix contacts in membrane proteins

As determined from the experimental approaches reported here, the very high correlation ($r = 0.94$, $p < 0.05$) (Fig. 4) of residue 'hydropathy' when measured for TM3/4 hairpins *vs.* TM4 peptides in the isotropic environment of a water/acetonitrile gradient on RP-HPLC indicates that segment hydropathy overwhelmingly dominates the partitioning of hydrophobic segments into non-polar microcompartments. In contrast, upon comparing the SDS-PAGE mobilities of the series of TM3/4 hairpins (Fig. 1A) with TM4 peptides (Fig. 5A), some intriguing differences are apparent (Fig. 5B). Firstly, we noted that TM4 SDS-PAGE migration rates for hydrophobic residues are similar in magnitude (highlighted in a yellow oval in Fig. 5B), while corresponding hairpins migrate over a significant range. These observations appear to suggest that the single strand helix effectively becomes saturated by bound detergent for all hydrophobic side chains — reinforcing the notion that the micelle can readily surround the single helix. Consistent with this suggestion, the same subset of residues at position 232 displayed the highest measured helical contents among CD spectra (Fig. 3). A scale reported for nonpolar phase helicity similarly indicates a corresponding group of residues of highest, closely spaced helical proclivities [19].

The implications of our findings with single strand TM4 peptides, in turn, act to clarify the folding characteristics displayed by the TM3/4 hairpin library. The fact that migration varies among the same group of hydrophobic residues (Fig. 5B) raises the possibility that many of the hairpins retain intra-hairpin contacts during SDS-PAGE experiments. The observed migration differences – that trend toward greater detergent binding for several hydrophobic mutants in the hairpins *vs.* the TM4 peptides – may thus reflect residue-dependent re-orientations of a TM3–TM4 van der Waals interface, thereby exposing varying faces of the hairpin helices to the SDS detergent in each mutant. This supposition is modeled in Fig. 6. Here, the wild type hairpin may retain tertiary contacts in SDS (Fig. 6A). A given mutation may preserve such helix–helix association, or do so by formation of an alternate van der Waals interface, causing rotation of (likely) both TM3 and TM4 segments around their major helical axes, thereby exposing different faces that in turn alter the measured extent of SDS binding (Fig. 6B). Alternatively, a local mutation may lead to dissociation of the helices that take on a 'necklace and bead structure' with independent – and likely increased – detergent–micelle interactions *vs.* the wild type hairpin (Fig. 6C). It is emphasized that our results provide no direct information on dynamic equilibria that may exist among the hairpin structures depicted in Fig. 6, and a given hairpin may consist of varying populations of species A, B, and/or C, which have been inferred based on the current work and previous biophysical and computational studies [10,20]. These sets of interactions would not arise in the monomeric single strand peptides, albeit detergent binding is similarly influenced by mutant-induced variations in peptide helicity and location within the micelle. Interestingly, the positively charged Lys and Arg are the only residues having much higher TM4 peptide mobility relative to where they fall among the hairpin series (Fig. 5B), a result that is best explained in the hairpins by the burial and interhelical interactions of Lys and Arg side chains with polar substituents on the TM3 helix, such as Gln-207 which is supported by the increased helicity of these constructs [9,10].

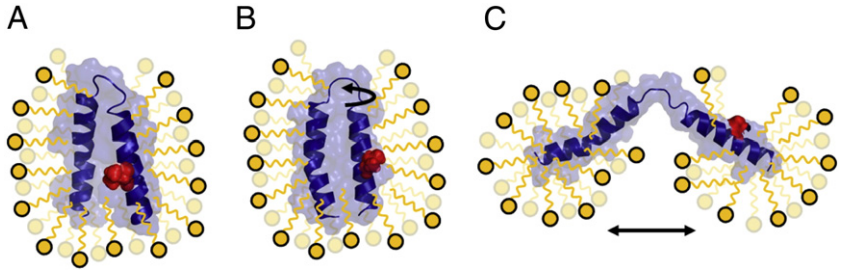

Fig. 6. Modeling the origin(s) of hairpin mobility variations due to helix–helix interactions. (A–C) Models of residue-dependent hairpin conformational interconversions that could explain differences in SDS-PAGE mobilities between the hairpins and the single strand TM4 peptides (Fig. 5B). Models were generated by PyMol [28]. The mutated position 232 is shown in red (as WT Val). (A) The hairpin is fully coated in detergent and favorable tertiary helix association is promoted. (B) A scenario where helix association is retained, but a particular mutation has caused TM4 (and/or TM3) to rotate about its major axis, creating a new helix–helix interface and thereby exposing different sets of residues to SDS. (C) A model of a mutant where the TM3 and TM4 helices have dissociated, and each helix may interact independently with the detergent micelles.

4.3. Effects of strongly polar residue substitutions on SDS-PAGE mobility depend on peptide context

Substitution of Val with the residues D, E, N, and Q at position 232 in the context of the TM4 peptide causes a mobility increase on SDS-PAGE. While this result is consistent with decreased hydrophobicity and/or SDS binding by the TM4 peptide, it contrasts with previous observations of polar residue substitutions in other single peptide models. For example, in the context of a 23-residue poly-Leu model TMD, a second, slowly-migrating band appears on SDS-PAGE when a single Leu is replaced with D, E, N, or Q, which was identified as a dimer stabilized by interhelical hydrogen bonding [21,22]. Swapping of Val for N at the 12th position of the 20-residue hydrophobic segment of the *de novo* designed peptide MS1 also decreased the SDS-PAGE mobility of this peptide such that its apparent MW was that of the dimeric species [23]. However, the decreased SDS-PAGE mobility of the Asn- *vs.* Val-substituted MS1 peptides has been attributed to a significant difference in their interactions with SDS [24]. The effects of polar residue substitutions on the SDS-PAGE mobility of peptides are therefore complex, and appear from these combined results to depend on the sequence background that hosts the polar residue replacement and/or peptide–SDS interactions; as such, we suggest that SDS-PAGE migration data should be confirmed by secondary methods.

5. Conclusion

The SDS-PAGE methodology described herein, in conjunction with the application of several complementary biophysical techniques, allow a residue-dependent analysis of how individual amino acid side chains in a membrane protein/peptide construct can influence local detergent (lipid) interactions — and how these interactions may directly influence tertiary helix–helix interactions. While residue hydrophobicity is consistently the dominant effect, mutant-mediated variations in interhelical folding can play a concurrent role in determining the conformation of a given hairpin–micelle (Fig. 6) complex and in turn how these single site mutations can lead to or influence the severity of a variety of diseases including cystic fibrosis, retinitis pigmentosa and type 2 diabetes [25—27]. Understanding the sequence-dependent nature of these processes is essential to determining the structural basis for disease-phenotypic mutations and ultimately what may be the best strategy to correct them. This work clearly describes the significant folding implications that can be brought about by a single mutation to a membrane-embedded protein. Future work will aim to elucidate the context dependence of these effects as the mutations' position within the helix is varied.

Acknowledgements

The authors wish to thank David Tulumello for helpful discussions, and Arianna Rath for critical reading and editing of the manuscript. This work was supported, in part, by grants to C.M.D. from the Canadian Cystic Fibrosis Foundation and from the Canadian Institutes of Health Research (CIHR FRN-5810). C.M.M. holds a graduate award from the CIHR Training program in Protein Folding & Interaction Dynamics: Principles and Diseases.

References

[1] G. Kuznetsov, S.K. Nigam, Folding of secretory and membrane proteins, N. Engl. J. Med. 339 (1998) 1688–1695.
[2] K. Enquist, M. Fransson, C. Boekel, I. Bengtsson, K. Geiger, L. Lang, A. Pettersson, S. Johansson, G. von Heijne, I. Nilsson, Membrane-integration characteristics of two ABC transporters, CFTR and P-glycoprotein, J. Mol. Biol. 387 (2009) 1153–1164.
[3] T. Hessa, H. Kim, K. Bihlmaier, C. Lundin, J. Boekel, H. Andersson, I. Nilsson, S.H. White, G. von Heijne, Recognition of transmembrane helices by the endoplasmic reticulum translocon, Nature 433 (2005) 377–381.
[4] T. Hessa, N.M. Meindl-Beinker, A. Bernsel, H. Kim, Y. Sato, M. Lerch-Bader, I. Nilsson, S.H. White, G. von Heijne, Molecular code for transmembrane-helix recognition by the Sec61 translocon, Nature 450 (2007) 1026–1030.
[5] S. Jaud, M. Fernandez-Vidal, I. Nilsson, N.M. Meindl-Beinker, N.C. Hubner, D.J. Tobias, G. von Heijne, S.H. White, Insertion of short transmembrane helices by the Sec61 translocon, Proc. Natl. Acad. Sci. U. S. A. 106 (2009) 11588–11593.
[6] S.H. White, W.C. Wimley, Membrane protein folding and stability: physical principles, Annu. Rev. Biophys. Biomol. Struct. 28 (1999) 319–365.
[7] M.B. Ulmschneider, M.S. Sansom, A. Di Nola, Properties of integral membrane protein structures: derivation of an implicit membrane potential, Proteins 59 (2005) 252–265.
[8] J.L. Popot, D.M. Engelman, Membrane protein folding and oligomerization: the two-stage model, Biochemistry 29 (1990) 4031–4037.
[9] C.M. Mulvihill, C.M. Deber, Evidence that the translocon may function as a hydropathy partitioning filter, Biochim. Biophys. Acta 1798 (2010) 1995–1998.
[10] A.G. Therien, F.E. Grant, C.M. Deber, Interhelical hydrogen bonds in the CFTR membrane domain, Nat. Struct. Biol. 8 (2001) 597–601.
[11] S. Peng, L.P. Liu, A.Q. Emili, C.M. Deber, Cystic fibrosis transmembrane conductance regulator: expression and helicity of a double membrane-spanning segment, FEBS Lett. 431 (1998) 29–33.
[12] R.A. Melnyk, A.W. Partridge, J. Yip, Y. Wu, N.K. Goto, C.M. Deber, Polar residue tagging of transmembrane peptides, Biopolymers 71 (2003) 675–685.
[13] M.D. Abramoff, P.J. Magelhaes, S.J. Ram, Image processing with ImageJ, Biophotonics Int. 11 (2004) 36–42.
[14] A. Rath, M. Glibowicka, V.G. Nadeau, G. Chen, C.M. Deber, Detergent binding explains anomalous SDS-PAGE migration of membrane proteins, Proc. Natl. Acad. Sci. U. S. A. 106 (2009) 1760–1765.
[15] H. Wehbi, G. Gasmi-Seabrook, M.Y. Choi, C.M. Deber, Positional dependence of non-native polar mutations on folding of CFTR helical hairpins, Biochim. Biophys. Acta 1778 (2008) 79–87.
[16] R.M. Johnson, K. Hecht, C.M. Deber, Aromatic and cation–pi interactions enhance helix–helix association in a membrane environment, Biochemistry 46 (2007) 9208–9214.
[17] R.M. Johnson, C.L. Heslop, C.M. Deber, Hydrophobic helical hairpins: design and packing interactions in membrane environments, Biochemistry 43 (2004) 14361–14369.
[18] D.V. Tulumello, C.M. Deber, Positions of polar amino acids alter interactions between transmembrane segments and detergents, Biochemistry 50 (2011) 3928–3935.
[19] C.M. Deber, C. Wang, L.P. Liu, A.S. Prior, S. Agrawal, B.L. Muskat, A.J. Cuticchia, TM Finder: a prediction program for transmembrane protein segments using a combination of hydrophobicity and nonpolar phase helicity scales, Protein Sci. 10 (2001) 212–219.
[20] P.J. Bond, J. Holyoake, A. Ivetac, S. Khalid, M.S. Sansom, Coarse-grained molecular dynamics simulations of membrane proteins and peptides, J. Struct. Biol. 157 (2007) 593–605.
[21] F.X. Zhou, H.J. Merianos, A.T. Brunger, D.M. Engelman, Polar residues drive association of polyleucine transmembrane helices, Proc. Natl. Acad. Sci. U. S. A. 98 (2001) 2250–2255.
[22] F.X. Zhou, M.J. Cocco, W.P. Russ, A.T. Brunger, D.M. Engelman, Interhelical hydrogen bonding drives strong interactions in membrane proteins, Nat. Struct. Biol. 7 (2000) 154–160.
[23] C. Choma, H. Gratkowski, J.D. Lear, W.F. DeGrado, Asparagine-mediated self-association of a model transmembrane helix, Nat. Struct. Biol. 7 (2000) 161–166.
[24] W.F. Walkenhorst, M. Merzlyakov, K. Hristova, W.C. Wimley, Polar residues in transmembrane helices can decrease electrophoretic mobility in polyacrylamide gels without causing helix dimerization, Biochim. Biophys. Acta 1788 (2009) 1321–1331.
[25] B. Kerem, J.M. Rommens, J.A. Buchanan, D. Markiewicz, T.K. Cox, A. Chakravarti, M. Buchwald, L.C. Tsui, Identification of the cystic fibrosis gene: genetic analysis, Science 245 (1989) 1073–1080.
[26] T.P. Dryja, T.L. McGee, E. Reichel, L.B. Hahn, G.S. Cowley, D.W. Yandell, M.A. Sandberg, E.L. Berson, A point mutation of the rhodopsin gene in one form of retinitis pigmentosa, Nature 343 (1990) 364–366.
[27] J.R. Brender, K. Hartman, K.R. Reid, R.T. Kennedy, A. Ramamoorthy, A single mutation in the nonamyloidogenic region of islet amyloid polypeptide greatly reduces toxicity, Biochemistry 47 (2008) 12680–12688.
[28] W.L. DeLano, The PyMOL Molecular Graphics System, DeLano Scientific, Palo Alto, CA, USA, 2008.